Available online at www.sciencedirect.com
SCIENCE DIRECT®
ELSEVIER
Journal of Solid State Chemistry 179 (2006) 849–854
JOURNAL OF SOLID STATE CHEMISTRY
www.elsevier.com/locate/jssc

Mixed crystals in the system $Cu_2MnGe_xSn_{1-x}S_4$: Phase analytical investigations and inspection of tetrahedra volumes

Thomas Bernert, Manfred Zabel, Arno Pfitzner*

Institut für Anorganische Chemie, Universität Regensburg, Universitätsstr. 31, D-93040 Regensburg, Germany

Received 10 November 2005; accepted 4 December 2005
Available online 9 January 2006

Abstract

Cu_2MnGeS_4 crystallizes orthorhombic in a wurtzite superstructure type while Cu_2MnSnS_4 crystallizes in a tetragonal sphalerite superstructure type. Lattice constants and thermal analyses of the solid solution series $Cu_2MnGe_xSn_{1-x}S_4$ are presented. A two-phase region is found from $Cu_2MnGe_{0.3}Sn_{0.7}S_4$ to $Cu_2MnGe_{0.5}Sn_{0.5}S_4$. The cell volume of the mixed crystals increases with increasing Sn content. The melting points increase smoothly with increasing Ge content to $x = 0.5$ and then steeply for higher Ge contents. The single crystal X-ray structure analysis of $Cu_2MnGe_{0.55}Sn_{0.45}S_4$ is presented. The refinement converges to $R = 0.0270$ and $wR_2 = 0.0586$, Z is 2. The volumes of the tetrahedra $[MS_4]$ (M = Cu, Mn, Ge, Sn) are calculated. From these volumes the differences in size of the tetrahedra are derived and compared with the corresponding differences in the end members of the solid solution series. It turns out that the resulting structure type in these materials depends on the volume differences of the constituting tetrahedra $[MS_4]$.

Keywords: Wurtzite superstructure type; Sphalerite superstructure type; Solid solution series; Quaternary compounds

1. Introduction

There is a strong interest in so-called tetrahedral compounds since many years because of their physical properties. The electrical properties of these semiconducting materials are under investigation as well as their optical and magnetical properties, e.g. [1–5]. Structural investigations led to valence electron rules that can be used for the prediction which compositions can form normal or defect tetrahedral compounds [6]. The cubic close packing of the anions in sphalerite and the hexagonal close anion packing in wurtzite are the most common among more than 200 known anion stacking variants in tetrahedral structures. An easy concept to predict or to explain the preference for one of these two structure types is not yet available because of the small energy difference between the two aristotypes.

Especially in the last years the research concentrated on the investigation of phase diagrams of quasi-ternary systems I_2Q–IIQ–IVQ_2 (I = Cu, Ag, II = Cd, Hg, Zn, IV = Si, Ge, Sn, Q = S, Se, Te) [7]. Quaternary compounds are formed in these systems and Rietveld refinements of several compounds of the type I_2–II–IV–Q_4 are available in literature. Back in the 1970s, Schäfer et al. already investigated many quaternary compounds of the I_2–II–IV–Q_4 type by X-ray powder diffraction [8]. They observed that many Sn-containing materials crystallize preferably in sphalerite superstructure types while the silicon-containing compounds crystallize in wurtzite superstructure types. The intervening germanium compounds show no clear preference for one of the two-anion packing variants. According to [7] to date mainly germanium compounds are found to have both, a high- and a low-temperature modification (e.g. Cu_2ZnGeS_4/Se_4, Cu_2CdGeS_4/Se_4). Usually the high-temperature modification is the wurtzite superstructure variant, as wurtzite is the high-temperature modification of ZnS itself [9]. Until the beginning of the 1990s the number of compounds containing tellurium as the anion or silver instead of copper was very small [10,11]. Some quaternary tellurides were described by Haeuseler et al. [12]. They also found solids of the composition Ag_2HgMQ_4 with M = Ge, Sn, and Q = S, Se

*Corresponding author. Fax: +49 941 943 4983.
E-mail address: arno.pfitzner@chemie.uni-regensburg.de (A. Pfitzner).

0022-4596/$ - see front matter © 2005 Elsevier Inc. All rights reserved.
doi:10.1016/j.jssc.2005.12.009

[13]. A quaternary compound containing Ag and Te was described by Wooley et al.: $Ag_2MnGeTe_4$ [14]. Contrary to the copper-containing quaternary materials in the quasi-ternary systems Ag_2Se–Zn(Cd, Hg)Se–$SiSe_2$ no compounds of the type I_2–II–IV–Se_4 are found [15,16].

Our interest in normal tetrahedral compounds was triggered by the observation that the sphalerite superstructure-type compound Cu_3SbS_4 shows a much smaller difference of the constituting distinct tetrahedra [MS_4] (M = Cu, P, Sb) than the wurtzite superstructure variant Cu_3PS_4 [17]. Therefore we started systematic investigations on tetrahedral compounds of different types [18]. The results underlined the expectations insofar as the tetrahedra distortions in wurtzite superstructure variants were more pronounced than the ones in sphalerite superstructure variants. Many compounds showed a clear preference but others fell in an overlap area where both structure types could occur principally. A similar idea was later presented by Parasyuk et al. [7] They discussed the influence of the different ionic radii of the cations and the correlated deformations of the different tetrahedra [MS_4] on the stability of the two principally different structural variants and even on the stability of the normal adamantane structures (see [6] for the definition of this term).

Continuing our systematic investigations of the tetrahedra volumes we recently analyzed the quaternary compounds Cu_2MnSiS_4, Cu_2MnGeS_4, and Cu_2MnSnS_4, i.e. we varied the M^{IV} ion [19]. The influence of the divalent metal on the preferred structure type was a subject of the investigations on $Cu_2Mn_xCo_{1-x}GeS_4$ [20]. Herein, we present mixed crystals in the system $Cu_2MnGe_xSn_{1-x}S_4$, i.e., we elucidate the stability range of the wurtzite and the sphalerite superstructure types with respect to the volume of the tetrahedra around the four-valent cation, and compare the tetrahedra volumes [MS_4] in $Cu_2MnGe_{0.55}Sn_{0.45}S_4$ with those of the end members.

2. Experimental

Mixed crystals $Cu_2MnGe_xSn_{1-x}S_4$ were prepared from the end members. Stoichiometric mixtures were ground intensely in an agate mortar, pressed to pellets, and brought to reaction at a temperature of 800 °C in evacuated sealed silica ampoules. The procedure was repeated after 5 days to ensure homogeneous products. The end members were prepared from high-purity elements as described in [19]. The purity of the products was confirmed by X-ray powder diffraction. The quality of the products improved during the second heating period. Powder data were collected on a STOE Stadi P (Ge monochromator, Cu$K\alpha_1$ radiation).

A single crystal of $Cu_2MnGe_{0.55}Sn_{0.45}S_4$ was fixed on a glass capillary for X-ray structure analysis. Diffraction data were collected on a STOE IPDS I equipped with a graphite monochromator and Mo$K\alpha$ radiation. A numerical absorption correction based on equivalents was performed. Details concerning data collection and structure refinement can be taken from Table 1. The single crystal refinement revealed a germanium content of x(Ge) = 0.553 (6) and a tin content of $1-x$(Sn) = 0.447 (6) assuming a fully occupied position with statistical disorder.

Table 1
Crystallographic data of $Cu_2MnGe_{0.55}Sn_{0.45}S_4$ [a]

Formula weight (g mol^{-1})	401.29
Crystal size (mm^3)	0.32 × 0.24 × 0.20
Color	Black
Crystal system	Orthorhombic
Space group	$Pmn2_1$
Lattice constants (Å) from powder data	$a = 7.680(2)$ $b = 6.577(1)$ $c = 6.292(1)$
Cell volume (Å^3), Z	317.8(1), 2
$\rho_{X\text{-ray}}$ (g cm^{-3})	4.242
Diffractometer	STOE IPDS, Mo$K\alpha$, $\lambda = 0.71073$ Å, graphite monochromator
Image plate distance (mm)	55
Irradiation time/image (min)	12
Flack parameter	−0.03 (2)
Absorption correction	Numerical, shape optimized with X-Shape [21]
No. of faces for crystal description	14
Temperature (°C)	20
hkl-range	$-10<h<10$ $-9<k<9$ $-8<l<8$
θ-range	$3.10 \leqslant \theta \leqslant 29.25$
No. of reflections, R_{int}, $R(\sigma)$	4684, 0.0672, 0.0330
No. of independent reflections	903
No. of parameters	45
Structure solution	SHELXS97 [22], direct methods
Structure refinement	SHELXL97 [23]
R ($I>2\sigma$); R (all reflections)[b]	0.0258, 0.0270
wR ($I>2\sigma$); wR (all reflections)[b]	0.0581, 0.0586
Weighting parameter a[b]	0.0363
GooF[b]	1.048
Extinction coefficient	0.019 (2)
Largest difference peaks $\Delta\rho_{max}$/e Å^{-3}, $\Delta\rho_{min}$/e Å^{-3}	0.843, −0.635

[a]Further details of the crystal structure investigation are available from the Fachinformationszentrum Karlsruhe, D-76344 Eggenstein-Leopoldshafen (Germany), fax: +49 7247 808 666, e-mail: crysdata@fiz-karlsruhe.de, referring to number CSD-416029, name of the authors and citation of the paper.

[b]Definition of R, wR, GooF, and weighting scheme:

$$R = \frac{\sum ||F_o| - |F_c||}{\sum |F_o|},$$

$$wR = \sqrt{\frac{\sum[w(F_o^2 - F_c^2)^2]}{\sum[w(F_o^2)^2]}},$$

$$\text{GooF} = \sqrt{\frac{\sum[w(F_o^2 - F_c^2)^2]}{n-p}},$$

$$w = 1/[\sigma^2(F_o^2) + (aP)^2],\ P = [\max(F_o^2, 0) + 2F_c^2]/3.$$

DTA measurements were performed on a Setaram TMA 92 16.18. Small amounts of finely grinded samples were put into evacuated quartz ampoules of 2 mm diameter and about 10 mm length. The samples were heated from room temperature to 1200 °C with a rate of 10 °C/min. Two heating cycles were carried out in order to examine the melting behavior.

3. Results and discussion

3.1. Lattice constants and miscibility gap

The orthorhombic structure type of Cu_2MnGeS_4 exists up to about 40% tin, that is $x = 0.6$. A two-phase region spreads from $0.3 \leqslant x \leqslant 0.5$, as can be estimated from the powder data. Mixtures from $x = 0.2$ to the pure Sn end member crystallize in the tetragonal system. Fig. 1 shows the evolution of the cell volumes of the materials with changing composition. The volumes decrease linearly with increasing germanium content.

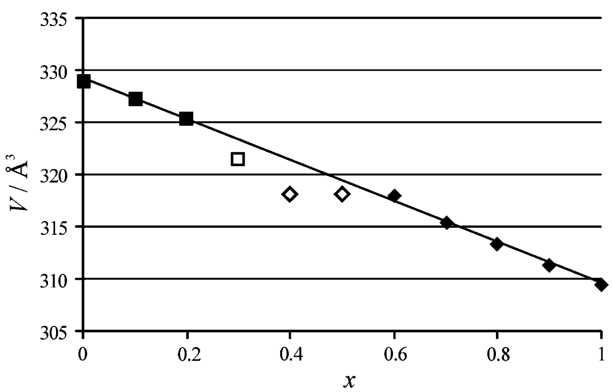

Fig. 1. Cell volumes vs. composition in the system $Cu_2MnGe_xSn_{1-x}S_4$. Empty symbols represent compositions that fall in the miscibility gap at 800 °C. ■ = Stannite type, ◆ = wurtzstannite type.

The lattice constants of the orthorhombic phases are plotted in Fig. 2. All three lattice parameters decrease linearly with increasing germanium content.

3.2. Thermal analysis

Compositions in the miscibility gap were heated to 920 °C in order to find out whether the width of the miscibility gap decreases with increasing temperature. The powder patterns indicate that the gap indeed decreases. While the powder diagram of $Cu_2MnGe_{0.5}Sn_{0.5}S_4$ heated to 800 °C clearly contains both phases, the tetragonal as well as the orthorhombic one, the tetragonal phase has disappeared in the pattern of the compound heated to 920 °C. However, we did not study the temperature dependence of the miscibility gap in detail.

The melting points of all compositions were determined by DTA measurements in order to obtain an idea of the melting behavior. Melting points for the end members can be found in Ref. [8]. Schäfer and Nitsche found 909 °C for Cu_2MnSnS_4 and 994 °C in the case of Cu_2MnGeS_4. The standard deviation is estimated to ± 5 °C. We obtained 907 °C for the tin compound and 1014 °C for Cu_2MnGeS_4 from onset points in the thermal measurements. For the latter value the difference to the literature is remarkably high. However, this discrepancy seems to be tolerable in this temperature range. In Fig. 3 the melting points are plotted against the germanium content. At $x = 0.5$ a kink is

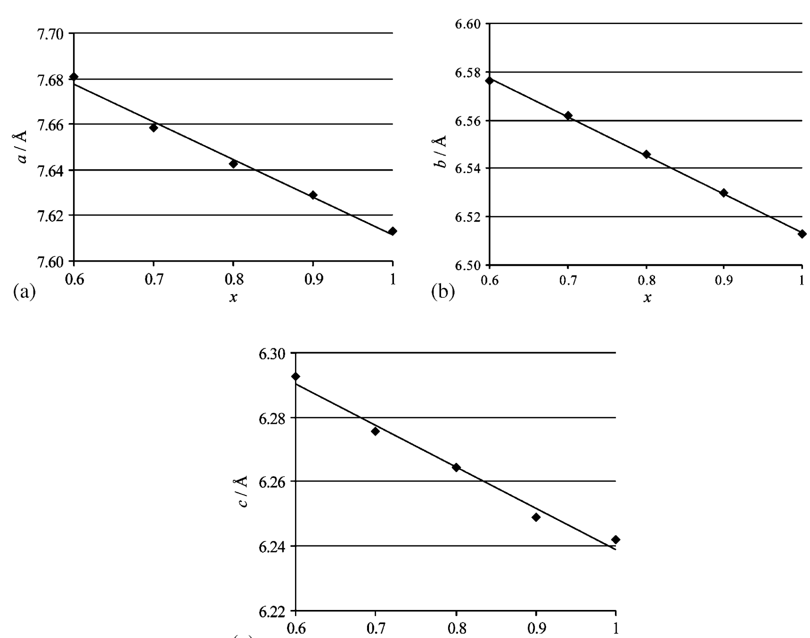

Fig. 2. (a) Lattice parameter a vs. the composition x. (b) Lattice parameter b vs. the composition x. (c) Lattice parameter c vs. the composition x.

observed. For small x the melting points increase linearly with a moderate gradient. From $x = 0.5$ to 1.0 the slope of the curve is steeper. It has to be pointed out that Fig. 3 does not represent a detailed phase diagram. Much more measurements and investigations were necessary for this purpose.

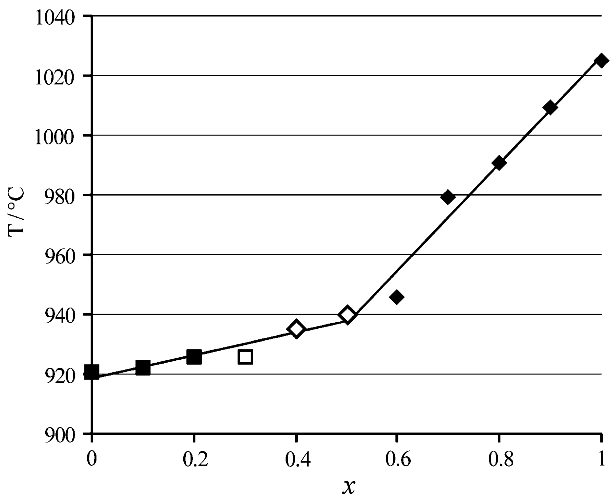

Fig. 3. Melting points vs. the germanium content of $Cu_2MnGe_xSn_{1-x}S_4$.

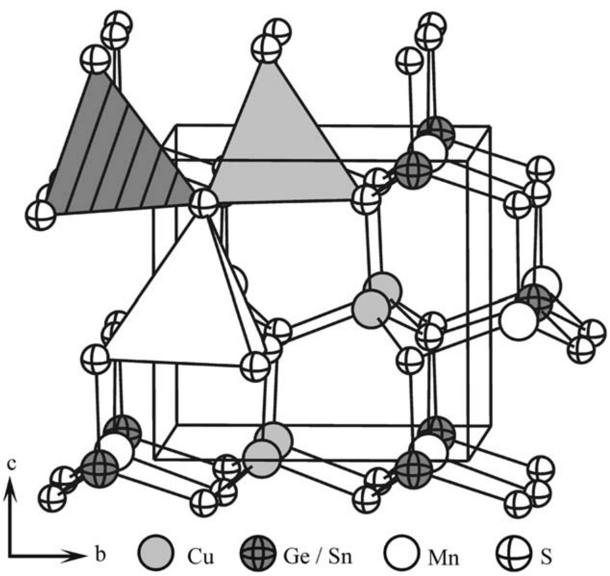

Fig. 4. Section of the crystal structure of $Cu_2MnGe_{0.55}Sn_{0.45}S_4$ along a. The tetrahedra $[CuS_4]$ (light gray) and $[(Ge_{0.55}Sn_{0.45})S_4]$ (gray, hatched) apparently have the same size.

Two heating cycles up to 1200 °C were carried out in order to detect incongruent melting. However, the melting points of all samples including the end members stayed unchanged in both cycles. So no evidence for incongruent melting or decomposition of the samples was found. High-temperature X-ray diffraction might help to elucidate the phase variation at high temperature and to obtain a complete phase diagram.

3.3. Single crystal investigations

The crystal structure of $Cu_2MnGe_{0.55}Sn_{0.45}S_4$ is depicted in Fig. 4. In Table 2 atomic positions are collected. Table 3 contains anisotropic displacement parameters and Table 4 summarizes distances and angles.

An inspection of the tetrahedra $[MS_4]$ in the *famatinite*-type compound Cu_3SbS_4 (cubic close packing, space group $I\bar{4}2m$) and in the wurtzite-type superstructure Cu_3PS_4 in [17] led to the assumption that wurtzite-type variants in general tolerate tetrahedra with quite different volumes while sphalerite-type superstructures are limited to small tetrahedra differences. In [18] we presented a concept how to obtain a quantitative measure of this thesis and gave examples.

In [19] we investigated the quaternary compounds Cu_2MnSiS_4, Cu_2MnGeS_4, and Cu_2MnSnS_4 with respect to their tetrahedra volumes. We agree with Parasyuk et al. who mentioned that the slight deformation of the tetrahedra $[GeS_4]$ is increased in the silicon compound and decreased in the case of tin [7].

Our quantitative concept is based on the volumes of the constituting tetrahedra of this class of compounds which can be derived from the following formula, Fig. 5:

$$V = \left(\frac{1}{288} \cdot \begin{vmatrix} 0 & r^2 & q^2 & a^2 & 1 \\ r^2 & 0 & p^2 & b^2 & 1 \\ q^2 & p^2 & 0 & c^2 & 1 \\ a^2 & b^2 & c^2 & 0 & 1 \\ 1 & 1 & 1 & 1 & 0 \end{vmatrix} \right)^{1/2}.$$

Table 2
Atomic positions and U^*_{eq} for $Cu_2MnGe_{0.55}Sn_{0.45}S_4$

Atom	Wyckoff pos.	Occ.[a]	x	y	z	U_{eq}[b]
Cu	4*b*	1.0	0.74933 (4)	0.67458 (5)	0.4756 (1)	0.0236 (2)
Mn	2*a*	1.0	0	0.16242 (8)	0.4684 (4)	0.0192 (2)
Sn	2*a*	0.447	0	0.82686 (4)	0.9689 (2)	0.0134 (1)
Ge	2*a*	0.553 (6)	0	0.82686 (4)	0.9689 (2)	0.0134 (1)
S1	2*a*	1.0	0	0.8162 (2)	0.3343 (2)	0.0177 (3)
S2	2*a*	1.0	0	0.1587 (2)	0.8554 (2)	0.0169 (3)
S3	4*b*	1.0	0.7590 (1)	0.6585 (1)	0.8417 (2)	0.0171 (2)

[a]An occupancy of 1.0 means a fully occupied site.
[b]U_{eq} is defined as one-third of the trace of the orthogonalized U_{ij} tensor.

Table 3
Anisotropic displacement parameters U_{ij} (in Å^2) for $Cu_2MnGe_{0.55}Sn_{0.45}S_4$

Atom	U_{11}	U_{22}	U_{33}	U_{23}	U_{13}	U_{12}
Cu	0.0242 (3)	0.0257 (3)	0.0210 (4)	0.0000 (3)	0.0003 (3)	−0.0013 (1)
Mn	0.0182 (3)	0.0202 (3)	0.0191 (4)	0.0014 (5)	0	0
Ge/Sn	0.0142 (2)	0.0135 (2)	0.0126 (2)	−0.0002 (2)	0	0
S1	0.0162 (5)	0.0168 (5)	0.0200 (7)	0.0028 (5)	0	0
S2	0.0163 (5)	0.0190 (5)	0.0158 (8)	−0.0013 (4)	0	0
S3	0.0186 (5)	0.0169 (4)	0.0159 (5)	0.0008 (3)	0.0001 (4)	0.0006 (2)

Table 4
Selected interatomic distances (in Å) and angles (in deg) for $Cu_2MnGe_{0.55}Sn_{0.45}S_4$

M–S1		2.300 (2)	S1–*M*–S2		109.86 (4)
M–S2		2.297 (1)	S1–*M*–S3	2 ×	109.47 (4)
M–S3	2 ×	2.300 (1)	S2–*M*–S3	2 ×	110.44 (4)
Mn–S1		2.428 (2)	S3–*M*–S3		107.13 (6)
Mn–S2		2.435 (3)			
Mn–S3	2 ×	2.446 (1)	S1–Cu–S2		111.64 (5)
Cu–S1		2.316 (1)	S1–Cu–S3		105.09 (5)
Cu–S2		2.333 (1)	S1–Cu–S3		112.01 (5)
Cu–S3		2.307 (2)	S2–Cu–S3		111.83 (5)
Cu–S3		2.348 (1)	S2–Cu–S3		107.44 (5)
			S3–Cu–S3		108.45 (4)
S1–Mn–S2		109.77 (9)			
S1–Mn–S3	2 ×	109.77 (7)			
S2–Mn–S3	2 ×	109.32 (6)			
S3–Mn–S3		108.87 (7)			

M represents the 2*a* position statistically occupied by Ge and Sn.

From all different volumes we calculate the average volume. Then we compute the deviation of each tetrahedron from the average value. The mean value of all these differences, the so-called $\overline{\Delta V_i}$, is used to quantify the differences of the tetrahedra in a normal adamantane structure. The values for Cu_2MnSiS_4, Cu_2MnGeS_4 and Cu_2MnSnS_4 are 11.1, 7.7 and 6.1, respectively [19]. The wurtzite-type superstructure compounds (M^{IV} = Si and Ge) have a bigger $\overline{\Delta V_i}$ than the sphalerite-type superstructure compound (M^{IV} = Sn). The difference between the germanium and tin compounds is quite small. Tetrahedra volumes [MS_4] of $Cu_2MnM^{IV}S_4$ (M^{IV} = Ge, ($Ge_{0.55}Sn_{0.45}$), Sn) are collected in Table 5. As the composition $Cu_2MnGe_{0.55}Sn_{0.45}S_4$ is close to a germanium content of 50% one might expect a $\overline{\Delta V_i}$ value somewhere in the middle between 7.7 and 6.1. However, the $\overline{\Delta V_i}$ value for $Cu_2MnGe_{0.55}Sn_{0.45}S_4$ is 6.1. This clearly indicates the limitation of this concept. As Ge and Sn statistically occupy a 2*a* position we cannot distinguish between the two ions. Therefore, the value for [($Ge_{0.55}Sn_{0.45}$)S_4] is an average value of [GeS_4] and [SnS_4] and this average value is close to the value of [CuS_4], see Table 5. The real local differences in size cannot be determined by X-ray diffraction. Therefore, the same $\overline{\Delta V_i}$ value as for tetragonal Cu_2MnSnS_4 is found.

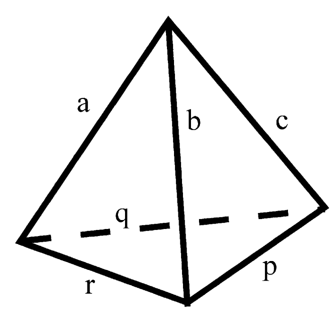

Fig. 5. General formula to compute tetrahedra volumes and labeling of tetrahedra edges [24].

The volumes for the [MS_4] tetrahedra lie on a straight line as shown in Fig. 6. The volume of [GeS_4] is 5.68 Å^3, and the one for [SnS_4] is 7.24 Å^3. As the volumes [(Ge_xSn_{1-x})S_4] can be linearly interpolated the value for $x = 55\%$ lies within these limits. It is 6.24 Å^3. This is close to the volume of the tetrahedron [CuS_4] (6.44 Å^3). That means there are three tetrahedra (2 × [CuS_4] and [($Ge_{0.55}Sn_{0.45}$)S_4]) in $Cu_2MnGe_{0.55}Sn_{0.45}S_4$ that have about the same size. Therefore $\overline{\Delta V_i}$ of $Cu_2MnGe_{0.55}Sn_{0.45}S_4$ is identical with $\overline{\Delta V_i}$ of Cu_2MnSnS_4 although the volume of [MnS_4] is remarkably greater than that of the other tetrahedra.

Table 5
Tetrahedra volumes of the compounds $Cu_2MnM^{IV}S_4$ in Å^3

Tetrahedron	Cu_2MnGeS_4	$Cu_2MnGe_{0.55}Sn_{0.45}S_4$	Cu_2MnSnS_4
CuS_4	6.44	6.44	6.42
MnS_4	7.53	7.45	7.50
$M^{IV}S_4$	5.68	6.24	7.24

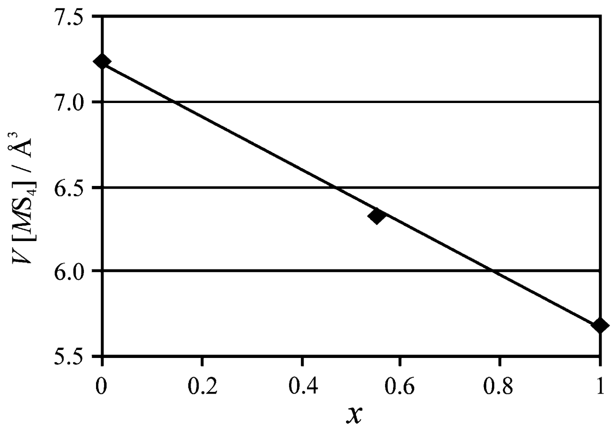

Fig. 6. Volumes of the tetrahedra MS_4 (M = Ge, Ge/Sn, Sn) vs. the composition.

Anyway, the $\overline{\Delta V_i}$ value for the Si compound is significantly bigger than for the other two materials. The fact that the compounds with Ge and Sn form mixed crystals also indicates a close relationship between their ionic radii and therefore for their similar tetrahedra volumes. These facts were observed similarly in the system Cu_3MS_4 (M = P, As, Sb). Cu_3AsS_4 and Cu_3SbS_4 form mixed crystals, too. The $\overline{\Delta V_i}$ value of the wurtzite superstructure-type compound Cu_3AsS_4 (5.2) is close to the value of the sphalerite superstructure variant Cu_3SbS_4 (3.3). The homologous compound Cu_3PS_4 does not form mixed crystals with Cu_3SbS_4 and its $\overline{\Delta V_i}$ value (10.3) is much bigger as compared to the As- and Sb-containing solids. [18]

Many quaternary tetrahedral compounds crystallize in two polymorphic modifications. The wurtzite modification usually is the high-temperature phase. For Cu_2MnGeS_4 we also found hints for a tetragonal modification at lower temperature. The lattice parameters are $a = 5.327(2)$ Å, $c = 10.431(4)$ Å and $V = 296.0(2)$ Å^3. Experiments to isolate the pure low-temperature phase at minor temperatures are subject of forthcoming studies.

Acknowledgments

We thank Christoph Mayer for some experimental help.

References

[1] H. Matsushita, T. Ichikawa, A. Katsui, J. Mater. Sci. 40 (2005) 2003.
[2] A. Caneschi, C. Cipriani, F. Di Benedetto, Phys. Chem. Miner. 31 (2004) 190.
[3] L. Guen, W.S. Glausinger, A. Wold, Mater. Res. Bull. 14 (1979) 463.
[4] D.M. Schleich, A. Wold, Mater. Res. Bull. 12 (1977) 111.
[5] L. Guen, W.S. Glausinger, J. Solid State Chem. 35 (1980) 10.
[6] E. Parthé, Wurtzite and sphalerite structures, in: J.H. Westbrook, R.L. Fleischer (Eds.), Crystal Structures of Intermetallic Compunds, Wiley, New York, 2000.
[7] O.V. Parasyuk, L.V. Piskach, Y.E. Romanyuk, I.D. Olekseyuk, V.I. Zaremba, V.I. Pekhnyo, J. Alloy Compd. 397 (2005) 85 and references therein.
[8] W. Schäfer, R. Nitsche, Z. Kristallogr. 145 (1977) 356.
[9] E.T. Allen, J.L. Crenshaw, H.E. Merwin, Am. J. Sci. 34 (1913) 341.
[10] M.M. Himmrich, Ph.D. Thesis, Universität Siegen, 1990.
[11] E. Parthé, K. Yvon, R.H. Deitch, Acta Crystallogr. B 25 (1969) 1164.
[12] H. Haeuseler, F.W. Ohrendorf, M. Himmrich, Z. Naturforsch. 46b (1991) 1049.
[13] H. Haeuseler, M. Himmrich, Z. Naturforsch. 44b (1989) 1035.
[14] J.C. Wooley, A.-M. Lamarche, G. Lamarche, C. Church, I.P. Swainson, T.M. Holden, J. Solid State Chem. 115 (1995) 192.
[15] O.V. Parasyuk, I.D. Oleksyuk, L.D. Gulay, L.V. Piskach, J. Alloy Compd. 354 (2003) 138.
[16] O.V. Parasyuk, L.D. Gulay, Ya.E. Romanyuk, I.D. Olekseyuk, J. Alloy Compd. 348 (2003) 157.
[17] A. Pfitzner, S. Reiser, Z. Kristallogr. 217 (2002) 51.
[18] A. Pfitzner, T. Bernert, Z. Kristallogr. 219 (2004) 20.
[19] T. Bernert, A. Pfitzner, Z. Kristallogr. 220 (2005) 968.
[20] T. Bernert, A. Pfitzner, Z. Anorg. Allg. Chem., in press.
[21] STOE und Cie GmbH Darmstadt, 1996, 1997, Crystal optimization for Numerical Absorption Correction.
[22] G.M. Sheldrick, SHELXS-97. Program for the Solution of Crystal Structures, University of Göttingen, Germany, 1997.
[23] G.M. Sheldrick, SHELXL-97. Program for the Refinement of Crystal Structures, University of Göttingen, Germany, 1997.
[24] I.N. Bronstein, K.A. Semendjaev, Taschenbuch der Mathematik, Verlag Harry Deutsch, Zürich, 1969.